EPJ Web of Conferences **113**, 02006 (2016)
DOI: 10.1051/epjconf/201611302006

Few-body, hyperspherical treatment of the quantum Hall effect

R. E. Wooten[1,a], K. M. Daily[1,2], and Chris H. Greene[1,b]

[1] *Purdue University Department of Physics and Astronomy 525 Northwestern Avenue, West Lafayette, Indiana 47907-2036*
[2] *Wolfram Research, Inc, 100 Trade Center Dr., Champaign, IL 61820*

Abstract. The quantum Hall effect arises from the quantum behavior of two-dimensional, strongly-interacting electrons exposed to a strong, perpendicular magnetic field [1, 2]. Conventionally treated from a many-body perspective, we instead treat the system from the few-body perspective using collective coordinates and the hyperspherical adiabatic technique developed originally for atomic systems [3]. The grand angular momentum K from K-harmonic few-body theory, is shown to be an approximate good collective quantum number in this system, and is shown to correlate with known fractional quantum Hall (FQH) states at experimentally observed filling factors.

1 Introduction

When electrons are confined to a finite, two-dimensional plane in the presence of a strong, perpendicular magnetic field, the measurements of the Hall resistance R_H are quantized to values of $h/\nu e^2$ when the filling factor ν takes on integer or certain rational fraction values. The filling factor ν is the number of occupied Landau levels in the non-interacting ground state of a finite-area system. The integer values of ν are well understood to arise from Landau level quantization, but the rational fraction values of ν arise entirely from electron correlations and remain a rich area of study.

In conventional treatments, the N-particle Hamiltonian is diagonalized in a single-particle defined Slater determinant basis, but in our treatment, we address the problem by transforming first to a set of collective coordinates and then transforming to a hyperspherical representation [4]. While its use in condensed matter physics has been limited, the adiabatic hyperspherical representation has been used successfully in a wide range of problems in few-body physics, including nuclear structure and reactivity, few-electron atoms, positron-electron systems, and Bose condensates. We assert that the technique can also effectively be applied to the many body quantum Hall system, and that it introduces an interesting and distinct framework for interpreting the system.

We begin by noting that the center of mass is separable in this system. The non-interacting relative coordinate Hamiltonian in units of the magnetic energy, $\hbar\omega_c = \hbar eB/m_e$, is

$$H_{\rm rel} = -\frac{1}{2\mu}\sum_{j=1}^{N_{\rm rel}} \boldsymbol{\nabla}_j^2 + \frac{\mu}{8}\sum_{j=1}^{N_{\rm rel}} \rho_j^2 + \frac{1}{2\hbar}\sum_{j=1}^{N_{\rm rel}} L_{z_j}^{\rm rel}, \tag{1}$$

[a] e-mail: wootenr@purdue.edu
[b] e-mail: chgreene@purdue.edu

where m_e is the effective electron mass in the material (typically low temperature gallium arsenide), B is the magnetic field, $\mu = (1/N)^{(1/N_{rel})}$ is a dimensionless mass scaling factor, N_{rel} is the number of relative coordinates, and the ρ_j are the relative coordinate lengths, which have been scaled by the magnetic length, $\lambda_0 = \sqrt{\hbar/m_e\omega_c}$.

2 Hyperspherical treatment

The relative coordinate Hamiltonian can be recast in terms of the hyperradius, R and a set of internal coordinates called the hyperangles (collectively referred to as $\mathbf{\Omega}$) that can be defined a number of arbitrary ways (e.g. see [5] or Appendix 4 of [6]) . The hyperradius defines a single length scale for the relative coordinates $R^2 = \sum_{j=1}^{N_{\rm rel}} \rho_j^2$, where the ρ_j are the Jacobi coordinates. In hyperspherical coordinates, the Hamiltonian is

$$H_{\rm rel} = -\frac{1}{2\mu}\boldsymbol{\nabla}^2_{R,\mathbf{\Omega}} + \frac{\mu}{8}R^2 + \frac{1}{2\hbar}L_z^{\rm rel,tot} + \kappa\frac{C(\mathbf{\Omega})}{R}, \tag{2}$$

where $\kappa = e^2/(4\pi\epsilon\lambda_0\hbar\omega_c)$ is the ratio of the magnetic to the Coulomb energy, ϵ is the dielectric constant of the material, and $C(\mathbf{\Omega})$ is the hyperangular form of the Coulomb interaction. $\boldsymbol{\nabla}^2_{R,\mathbf{\Omega}}$ is the Laplacian in hyperspherical coordinates,

$$\boldsymbol{\nabla}^2_{R,\mathbf{\Omega}} = \frac{1}{R^{2N_{\rm rel}-1}}\partial_R R^{2N_{\rm rel}-1}\partial_R - \frac{\hat{\boldsymbol{K}}^2}{R^2}, \tag{3}$$

where $\hat{\boldsymbol{K}}$ is the grand angular momentum operator. The eigenstates of $\hat{\boldsymbol{K}}^2$ are the hyperspherical harmonics $\Phi_{Ki}(\mathbf{\Omega})$, where

$$\hat{\boldsymbol{K}}^2\Phi^{(M)}_{Ki}(\mathbf{\Omega}) = K(K+2N_{\rm rel}-2)\Phi^{(M)}_{Ki}(\mathbf{\Omega}). \tag{4}$$

The i subscript here is a label indicating distinct, orthogonal functions that share K and M..

In the absence of the Coulomb interaction, each eigenfunction of Eq. 2 is separable into a product of a hyperradial function $F^{(M)}_{n_R K}(R)$ times an antisymmetrized hyperspherical harmonic, $\Phi^{(M)}_{Ka}(\mathbf{\Omega})$. Both the relative azimuthal angular momentum M and the grand angular momentum K are good quantum numbers in the non-interacting system, n_R is a hyperradial quantum number, and the index a distinguishes antisymmetric linear combinations of hyperspherical harmonic basis functions within the same K, M manifold. The non-interacting Schödinger equation simplifies to a one-dimensional, uncoupled ordinary differential equation,

$$\left\{-\frac{1}{2\mu}\frac{d^2}{dR^2} + U^{(M)}_K(R) - E\right\}F^{(M)}_{n_R K}(R) = 0, \tag{5}$$

where the noninteracting potentials $U^{(M)}_K(R)$ are given by

$$U^{(M)}_K(R) = \frac{(K+N_{\rm rel}-1/2)(K+N_{\rm rel}-3/2)}{2\mu R^2} + \frac{\mu}{8}R^2 + \frac{1}{2}M. \tag{6}$$

The non-interacting potential curves for the four particle system are shown in Fig. 1, where the lowest-lying curves each have $K = |M|$ and are the potentials for the lowest Landau level. These non-interacting solutions can be directly connected to the central parameter of the quantum Hall problem, the filling factor ν. In a typical 3-dimensional system, the hyperradius defines a characteristic "size" of a particle distribution, but in the case of particles on a plane, it defines an approximate area for a few

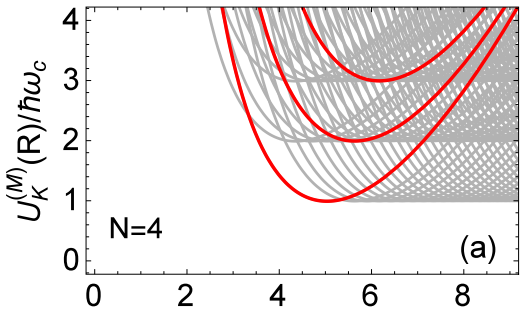

Figure 1. Light solid lines show the adiabatic potential curves of the noninteracting four-body system whose minima lie below $4\hbar\omega_c$. The lowest group ($K = |M|$) represents the lowest Landau level. The next and next-next higher groups are for $K = |M| + 2$ and $K = |M| + 4$, respectively. The dark solid lines are for $M = -6$, the lowest of which supports the integer quantum Hall state.

particle distribution. The hyperradial maxima of the ground states of the non-interacting hyperradial solutions, $F^{(M)}_{n_R K}(R)$ with $n_R = 0$, give characteristic hyperradii, and thus characteristic areas of the ground state solutions as a function of K. The characteristic areas leads to an expression for the hyperspherical filling factor in terms of only the particle number and the grand angular momentum,

$$\nu = \frac{N(N-1)}{2K}, \tag{7}$$

which connects the hyperspherical picture to the observations in the quantum Hall system.

With the introduction of the Coulomb interaction, the solutions become only approximately separable, and although M remains a good quantum number, K is only an approximate quantum number. We assume the solutions to the Schödinger equation that depend parametrically on the hyperradius, R,

$$\Psi(R, \mathbf{\Omega}) = R^{-N_{\rm rel}+1/2} \sum_{\chi} F^{(M)}_{E\chi}(R)\Phi^{(M)}_{\chi}(R; \mathbf{\Omega}), \tag{8}$$

where the subscript χ labels each channel, and the channel functions $\Phi^{(M)}_{\chi}(R; \mathbf{\Omega})$ are orthonormal for a fixed hyperradius. The potentials, $U^{(M)}_{\chi}(R)$, are found by diagonalizing the adiabatic Hamiltonian,

$$H_{ad}\Phi^{(M)}_{\chi}(R; \mathbf{\Omega}) = U^{(M)}_{\chi}(R)\Phi^{(M)}_{\chi}(R; \mathbf{\Omega}), \tag{9}$$

while treating the hyperradius as an adiabatic parameter and expanding the hyperangular channel functions at each hyperradius in terms of the antisymmetrized hyperspherical harmonics,

$$\Phi^{(M)}_{\chi}(R; \mathbf{\Omega}) = \sum_{Ka} c_{Ka}(R)\Phi^{(M)}_{Ka}(\mathbf{\Omega}). \tag{10}$$

As an example, the adiabatic potential curves for four particles with $M = -18$ and $\kappa = 1$ are shown in Fig. 2.

While an exact solution would include all adiabatic coupling between differing channel functions, in this system, coupling between different manifolds is weak, as shown for four particles in Fig.3 by the scaled adiabatic potentials $g^{(M)}_{\chi}(R)$,

$$g^{(M)}_{\chi}(R) = R^2\left(U^{(M)}_{\chi}(R) - \left[\frac{\mu}{8}R^2 - \frac{M}{2}\right]\right). \tag{11}$$

With the scaling shown in Fig. 3, the avoided crossings indicating inter-channel coupling can be seen, but most appear diabatic in nature. In addition, the avoided crossings appear only at much higher values of the hyperradius ($\kappa R \gtrsim 30\lambda_0$), whereas the noninteracting hyperradial wave function

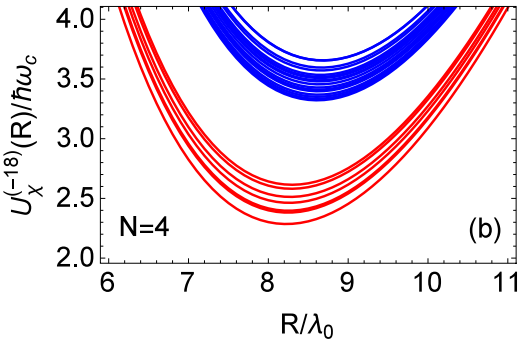

Figure 2. Adiabatic potentials $U_\chi^{(-18)}(R)$ for $N = 4$ particles, $M = -18$ and $\kappa = 1$. The larger gaps (on the order of $\hbar\omega_c$) indicate magnetic excitations, while the smaller splittings are due to Coulomb interactions. The separate clusters of curves indicate different K manifolds, with $K = |M|$ for the lowest grouping of curves and K increasing from bottom to top.

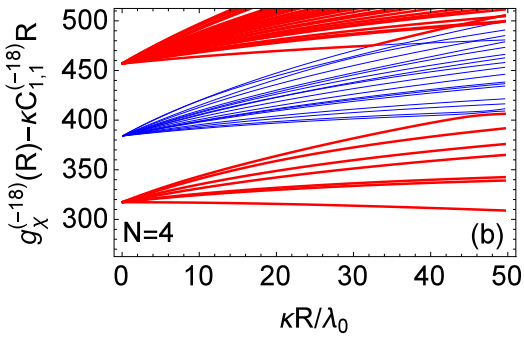

Figure 3. Bottom: $N = 4$ particles scaled adiabatic potentials $g_\chi(R)$ shifted by the smallest eigenvalue $C_{1,1}^{18}$ from diagonalizing the Coulomb interaction in the $K = |M| = 18$ manifold. Each bundle of curves originating from a higher point on the $\kappa R/\lambda_0$ axis corresponds to a higher K manifold. Avoided crossings indicating inter-channel coupling can be seen, but most are diabatic in nature and appear at hyperradii much larger than the typical scale of the system. That the majority of curves lack apparent adiabatic coupling indicates that the adiabatic approximation is particularly good in this system.

is contained within $R < 10.25\lambda_0$. Because the non-adiabatic coupling between manifolds is weak for the predominant hyperradial region, neglecting coupling between different K, M manifolds is a good approximation in this system.

Another indicator that the adiabatic approximation is particularly good is the fact that the upper and lower bounds in the hyperspherical representation differ by less than 10^{-4} in tested cases. By comparison, the ground state energies of the hydrogen negative ion differed by 1.7% in the upper and lower bounds in this approximation [7]. The impressive precision in the quantum Hall problem arises because the charged particles do not experience any attractive potentials, in contrast to the H^- system, where the attractive potentials cause potential valleys with much stronger deviations from adiabaticity.

In the absence of inter-K, M manifold coupling, the ground state energies can be found in a two-step process by first diagonalizing the Coulomb interaction within a hyperangular K, M basis then solving the hyperradial Schrödinger's equation numerically for varying magnetic fields. The ground state energies for the lowest Landau level, $K = |M|$ manifolds in a 6-particle system are shown in Fig. 4. The left-most curve corresponds to the 6-particle integer quantum Hall state, and the filling factor decreases towards the right as the magnetic field increases until slightly beyond the $\nu = 1/3$ Laughlin filling. The ground states at $\nu = 1$ and $\nu = 1/3$ filling are shown in red while ground states with $\nu = 2/3$ and $2/5$ are highlighted in blue. Other K, M manifold ground states that are also a ground state of the complete system at some values of the magnetic field are shown in green, and the remaining ground states are shown in black. The low energy states in this system other than the integer, Laughin, and Jain states are not identified, and their nature and properties are not predicted here.

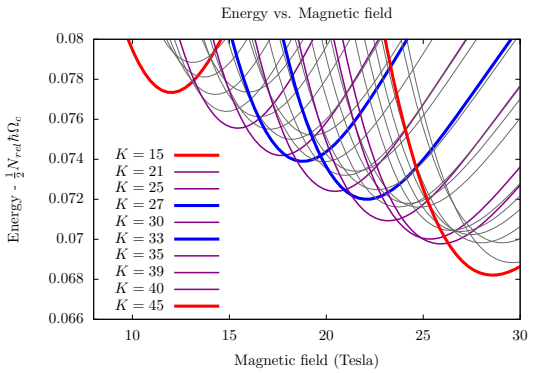

Figure 4. The ground state energies of K, M manifolds in the lowest Landau level (where $K = |M|$) as a function of the magnetic field, using experimental parameters matching a cold gallium arsenide system. These energies are found by first diagonalizing the Coulomb interaction in the hyperangular $K = |M| =$ bases, then solving the hyperradial Schrödinger's equation numerically with a restricted maximum hyperradius. The zero-point energies have been subtracted for scale. The curves for $K = 15, 27, 33, 45$ give the ground state energies of the $\nu = 1, 2/3, 2/5, 1/3$ quantum Hall states, respectively. Other states that are ground states of the system at some magnetic fields, but are not identified FQH states, are shown in purple, and the remaining higher energy states are shown in grey.

3 Exceptional degeneracy

One benefit of describing the system in hyperspherical coordinates is that the set of antisymmetrized hyperspherical harmonics in any K, M manifold forms a complete basis in the absence of interactions, and to a good approximation, is uncoupled to other K, M manifolds even in the presence of moderately strong Coulomb interactions. As such, it is interesting to consider the consequences of degeneracy on the individual manifolds without regard to the specific form of the interparticle interactions. As is well known from perturbation theory, introducing interactions into a degenerate manifold lowers the energy of the ground state relative to higher energy states, and the presence of additional degeneracy in the system strengthens this effect. As a result, it should be expected in this system that K, M manifolds with exceptionally high degeneracy relative to neighboring manifolds should also exhibit an enhanced energy gap between the ground state and excited states when interactions are introduced. As a dramatic energy gap is one of the primary requirements for a quantum Hall state, we predict that K, M manifolds with exceptional degeneracy are also likely to support quantum Hall states.

In the lowest Landau level ($K = |M|$), the degeneracy of each manifold can be determined analytically using group theoretical considerations. The degeneracies of the manifolds generally increase with $|M|$, but the relative change in degeneracy can be measured by enclosing the degeneracy function with an upper and lower envelope. Measuring the absolute degeneracy in comparison to the local height between the envelope functions gives a value for the relative degeneracy. In Fig. 5 we show a plot of the relative degeneracies of high degeneracy manifolds for a 6 particle system. The plot labels manifolds that support Laughlin and Jain states with their filling factors. All known Laughlin and Jain states in the 6-body system within the displayed $|M|$ range exist in manifolds with exceptionally high degeneracy, are labeled on this plot. The Laughlin and Jain fillings also display prominent degeneracy at significantly values of M, as well, and this trend has held true for systems with fewer particles, as well.

As can be seen in Fig. 5, while the integer, Laughlin, and Jain states display high relative degeneracy, this is not necessarily the case with other low energy states, and as such, the correlation between exceptional degeneracy and low energy ground states, which though suggestive, is not strict.

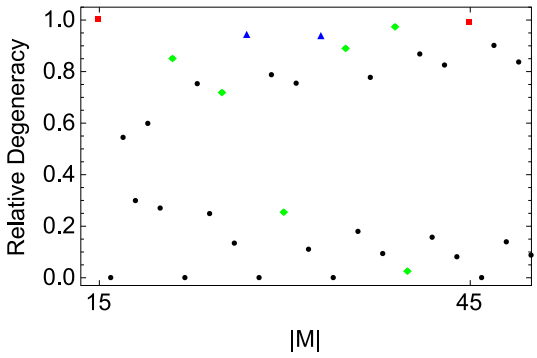

Figure 5. Relative degeneracies for the six-body system are shown as a function of $|M|$. Red squares show the integer quantum Hall effect $\nu = 1$ and the Laughlin $\nu = 1/3$ supporting manifolds; blue triangles show the Jain manifolds ($\nu = 2/3, 2/5$) that can exist in a 6 particle system; the green diamonds highlight manifolds that are ground states in Fig. 4, and the remaining black circles show the remaining K, M manifolds' relative degeneracies.

4 Conclusions

In this early study, we demonstrate that the adiabatic hyperspherical approximation from few-body theory is an appropriate framework from which to examine the complex many-body behavior of the quantum Hall system. In addition, the adiabatic hyperspherical approximation provides a new and different interpretation of the problem. In addition to the description of exceptional degeneracy, we expect that this approach will lead to other insights into the system's behavior that have been overlooked in the conventional many-body approach.

Acknowledgements

This work has been supported in part by a Purdue University Research Incentive Grant from the Office of the Vice President for Research. Some calculations were performed under resources from an NSF XSEDE allocation.

References

[1] D. C. Tsui, H. L. Stormer, A. C. Gossard, Phys. Rev. Lett. **48**, 1559 (1982).
[2] H. L. Stormer, D. C. Tsui, and A. C. Gossard, Rev. Mod. Phys. **71**, S298 (1999).
[3] J. Macek, J. Phys. B **1**, 831 (1968).
[4] K. M. Daily, R. E. Wooten, and Chris H. Greene, Phys. Rev. B **92**, 125427 (2015)
[5] Y. F. Smirnov and K. V. Shitikova, Sov. J. Part. Nucl. **8**, 44 (1977)
[6] S. T. Rittenhouse, J. von Stecher, J. P. D'Incao, N. P. Mehta, and C. H. Greene, Journal of Physics B: Atomic Molecular and Optical Physics **44**, 172001 (2011).
[7] H. Klar and M. Klar, Phys. Rev. A **17**, 1007 (1978).